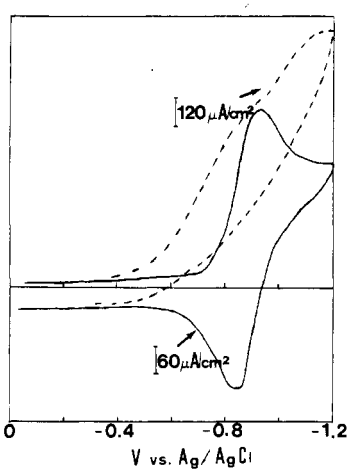

Figure 12. Cyclic voltammogram (200 mV/s) for a GC/poly-Co(*p*-NMe_2)TPP film ($\Gamma = 1.4 \times 10^{-9}$ mol/cm^2) in a CH_3CN + 0.1 M Et_4NClO_4 solution (solid curve) and for the same solution after addition of 2 volumes of H_2O (dashed curve).

potentials for O_2 reduction and larger slope. The slope for poly-Co(*o*-NH_2)TPP in 1 M NaOH is in fact very close to the four-electron value; we have confirmed by the rotating ring-disk technique[14] that this situation produces virtually no H_2O_2 product.

Assuming (as we have[14]) that the two waves for poly-Co(*o*-NH_2)TPP reflect monomeric and dimeric species in the film, then the lower activity of the other cobalt porphyrins may be connected to their lower dimerization constants, as found for Co(*p*-OH)TPP and Co(*p*-pyr)TPP solutions from absorbance spectroscopy (Table II).

Finally, Spiro et al.[24b] showed that Co(I) porphyrins placed in solutions and adsorbed or bound to GC electrodes[34] react rapidly with water. Figure 12 shows a test for water reduction using an electropolymerized poly-Co(*p*-NMe_2)TPP film (GC electrode). Co(II/I) voltammetry of the film in dry 0.1 M Et_4NClO_4/CH_3CN (solid curve) occurs at $E^{\circ\prime} = -0.92$ V, whereas upon addition of two volumes of water (dashed curve), an irreversible, split (ca. −0.68 and −1.01 V) wave, with greatly enhanced cathodic current and no reverse anodic wave, is observed. While it is reasonable to suppose that these waves represent H_2 evolution, they are not very stable (as Spiro[34] also experienced) and gradually decayed. No further studies were done. This instability is not characteristic of the polymeric porphyrin films in dry solvent, which in the potential window 0 to −1.5 V are very stable to repeated potential cycling.

Acknowledgment. This research was supported in part by a grant from the National Science Foundation.

(34) Kellet, R. M.; Spiro, T. G. *Inorg. Chem.* **1985**, *24*, 2378.

Contribution from the Department of Chemistry, University of Arizona, Tucson, Arizona 85721, and Chemistry Department, University of Manchester, Manchester M13 9PL, England

Syntheses, Structures, and Spectroscopic Properties of Six-Coordinate Mononuclear Oxo-Molybdenum(V) Complexes Stabilized by the Hydrotris(3,5-dimethyl-1-pyrazolyl)borate Ligand

W. E. Cleland, Jr.,[1a] Kerry M. Barnhart,[1a] Katsumoto Yamanouchi,[1a] David Collison,[1b] F. E. Mabbs,[1b] R. B. Ortega,[1a] and John H. Enemark*[1a]

Received September 5, 1986

A series of 19 mononuclear oxomolybdenum(V) compounds of the general formula LMoOXY (L = hydrotris(3,5-dimethyl-1-pyrazolyl)borate; (X,Y) = Cl^-, NCS^-, N_3^-, OR^-, SR^-, and the dianions of ethylene glycol, mercaptoethanol, dimercaptoethane, catechol, *o*-mercaptophenol, *o*-aminophenol, *o*-aminobenzenethiol, and toluenedithiol) have been prepared and characterized by electron paramagnetic resonance spectroscopy (EPR), cyclic voltammetry, UV–visible spectroscopy, and mass spectrometry. The $LMoO(SR)_2$ complexes possess the cis sulfur ligands proposed for the molybdenum cofactor. The structure of $LMoO(SPh)_2$ was determined by X-ray crystallography: space group $P2_1/c$, $Z = 4$, $a = 13.079$ (6) Å, $b = 14.438$ (7) Å, $c = 15.836$ (9) Å, $\beta = 104.73$ (4)°. The molecule adopts the expected *fac* six-coordinate stereochemistry with cis thiolate groups. The average Mo–S distance is 2.382 (2) Å, and the average Mo–O distance is 1.676 (4) Å. The Mo–N distances range from 2.164 (5) to 2.357 (5) Å. The isotropic $\langle g \rangle$ and $\langle A \rangle$(^{95,97}Mo) values show an inverse correlation and cluster according to the nature of the donor atoms. Sulfur donor atoms lead to large $\langle g \rangle$ and small $\langle A \rangle$ values. The anisotropies of the *g* values for $LMoO(OR)_2$ and $LMoO(SR)_2$ complexes show marked differences between monodentate and chelated ligands. All LMoOXY complexes undergo reversible one-electron reductions. The reduction potentials span a range of 1.3 V depending upon the nature of X and Y; $LMoO(NCS)_2$ is most easily reduced, and $LMoO(OCH_2CH_2O)$ is the most difficult to reduce. Complexes become easier to reduce as alkoxide groups are replaced by thiolate groups.

Introduction

Molybdenum is an essential trace element which is found in enzymes such as xanthine oxidase, sulfite oxidase, and nitrate reductase.[2,3] The chemical reactions catalyzed by these enzymes all involve a change in the number of oxygen atoms in the substrate, and there is strong evidence that these enzymes possess a common molybdenum cofactor (I).[4,5] EXAFS studies support

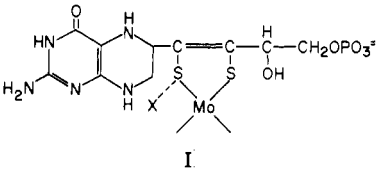

I

a mononuclear molybdenum center with at least two RS^- ligands bound to the molybdenum atom.[6,7]

An overall chemical reaction cycle for oxo–molybdenum centers of such enzymes involving Mo(IV), Mo(V), and Mo(VI) is shown

(1) (a) University of Arizona. (b) University of Manchester.
(2) Spence, J. T. *Coord. Chem. Rev.* **1983**, *48*, 59–82.
(3) *Molybdenum and Molybdenum-Containing Enzymes*; Coughlan, M. P., Ed.; Pergamon: New York, 1980.
(4) Johnson, J. L.; Rajogopalan, K. V. *Proc. Natl. Acad. Sci. U.S.A.* **1982**, *79*, 6856–6860.
(5) Cramer, S. P.; Stiefel, E. I. In *Molybdenum Enzymes*; Spiro, T. G., Ed.; Wiley: New York, 1985; Chapter 8, pp 411–441.
(6) (a) Cramer, S. P.; Wahl, R.; Rajagopalan, K. V. *J. Am. Chem. Soc.* **1980**, *103*, 7721–7727. (b) Bordas, J.; Bray, R. C.; Garner, C. D.; Gutteridge, S.; Hasnain, S. S. *Biochem. J.* **1980**, *191*, 499–508.
(7) Cramer, S. P. *Adv. Inorg. Bioinorg. Mech.* **1983**, *2*, 259–316.

0020-1669/87/1326-1017$01.50/0

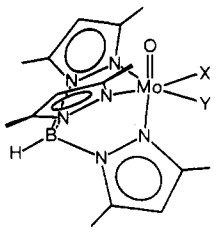

X,Y = Cl^-, SR^-, OR^-, NCS^-, N_3^-

(1-X,Y) ◻ $^-XCH_2CH_2Y^-$; X,Y ◻ O,S

(2-X,Y) = $^-XC_6H_4$-o-Y^-; X,Y = O,S,NH

Figure 1. Stereochemistry of LMoOXY, LMoO(1-X,Y), and LMoO(2-X,Y) complexes and ligand abbreviations.

Scheme I

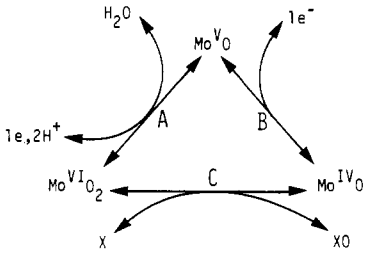

in Scheme I. Several chemical models for the oxo-transfer reaction between Mo(IV) and Mo(VI), represented by C of Scheme I, have been demonstrated.[8-10] Our interest has been in the EPR-active Mo(V) species shown at the top of Scheme I. The EPR signals of these Mo(V) states are observed upon reduction of the enzyme with substrate or dithionite and are usually present in equilibrium with both Mo(IV) and Mo(VI).[11] The Mo(V) signal appears within milliseconds after addition of a reducing agent, and its form is time-dependent. Kinetics measurements[11] have shown that the Mo(V) states are sufficiently long lived to be intermediates in the catalytic cycle. Rapid-freezing methods[11] have been important in obtaining information about the earliest stages of development of the EPR signal. However, the absence of crystal structures of molybdoenzymes makes detailed interpretation of the enzyme EPR spectra difficult. Consequently, present descriptions of the coordination environment of the molybdenum centers in enzymes rest upon comparisons of spectra obtained from the enzymes with those of well-characterized molybdenum complexes.

The isolation and characterization of Mo(V) complexes that may be synthetic analogues of the Mo(V) states in enzymes are difficult because of the propensity of oxo–Mo(V) complexes to form binuclear diamagnetic products in the presence of trace amounts of water. Our approach to this problem has been to create a steric pocket for the molybdenum atom in order to inhibit such dimerization reactions. A simple pocket-shaped ligand is hydrotris(3,5-dimethyl-1-pyrazolyl)borate, L. Complexes of this ligand were extensively studied by Trofimenko,[12] who first isolated the oxo–Mo(V) complex $LMoOCl_2$.[13] We have developed an improved synthetic route to $LMoOCl_2$ and to related mononuclear oxo–Mo(V) complexes. Figure 1 shows the stereochemistry of the complexes and the ligand abbreviations. Several of the complexes in Figure 1 contain two cis sulfur ligands, as proposed for the molybdenum cofactor (I).[4] This report[14] describes the preparation of these complexes and their characterization by EPR spectroscopy, X-ray structure determination, and other physical methods. Related mononuclear diamagnetic dioxomolybdenum(VI) complexes of the type $LMoO_2X$ have also been prepared[14c] and characterized by ^{95}Mo NMR.[14d]

Experimental Section

Reactions were carried out under an atmosphere of pure dry argon; solvents were thoroughly degassed before use. Subsequent workup was carried out in air. Solvents were purified by distillation: tetrahydrofuran from sodium benzophenone; 1,2-dichloroethane and dichloromethane from P_2O_5; acetonitrile from calcium hydride; toluene from sodium; hexanes and pentanes from sodium hydride. Potassium hydrotris(3,5-dimethyl-1-pyrazolyl)borate (KL) was prepared by the literature method.[15] Silica gel 60 used in adsorption chromatography was obtained from Fluka Chemical Co. Molybdenum pentachloride was obtained from Aldrich Chemical Co. The purity of isolated compounds as well as the progress of the reactions was monitored by thin-layer chromatography. Analyses were performed by Atlantic Microlab Inc., Atlanta, GA.

Preparation of $LMoOCl_2$. To 16.4 g (60 mmol) of $MoCl_5$ in a 200-mL airless flask at −77 °C was slowly added 120 mL of tetrahydrofuran (also at −77 °C) with vigorous stirring. The reaction mixture was gradually brought to room temperature with continuous stirring. Near room temperature an exothermic reaction began, the color changed from dark red-brown to green, and a green precipitate subsequently formed. To the resulting slurry was added 20 g (59.5 mmol) of KL, and the mixture was heated at 50 °C for 12 h with stirring. The resultant green precipitate was separated from the dark red supernatant by filtration, washed several times with acetonitrile, and dried in vacuo. The crude product was dissolved in ~1 L of refluxing 1,2-dichloroethane, and the solution was filtered to remove potassium chloride and evaporated to dryness in vacuo. The green product was washed with acetonitrile several times to remove a red impurity and then dried in vacuo. The yield was 20 g (70%) based on Mo. A sample for elemental analysis was obtained by recrystallization from 1,2-dichloroethane. Anal. Calcd for $C_{15}H_{22}N_6OCl_2BMo$: C, 37.53; H, 4.62; N, 17.51; Cl, 14.77. Found: C, 37.53; H, 4.64; N, 17.47; Cl, 14.81. IR: ν(MoO) 960 cm^{-1}.

Preparation of LMoOXY, LMoO(1-X,Y), and LMoO(2-X,Y). These complexes were prepared by one of three methods. The general procedure for each is described below. Purified complexes were stored under dinitrogen.

Methods 1 and 2. From $LMoOCl_2$. To a slurry of 2 g (4.2 mmol) of $LMoOCl_2$ in 50 mL of toluene at 70 °C was added either a mixture of 0.6 mL (8.4 mmol) of triethylamine and 8.4 mmol of HX (the appropriate alcohol or thiol) (method 1) or 8.4 mmol of NaX (method 2) in 5 mL of toluene. Reactions were monitored by TLC. Upon completion the reaction mixture was cooled to room temperature, filtered, and evaporated to dryness in vacuo (unless otherwise stated) and the product then either chromatographed on silica gel or recrystallized as described below.

Method 3. From LMoO(1-O,O). To a slurry of 2.0 g (4.2 mmol) of LMoO(1-O,O) (vide infra) in 50 mL of toluene at 70 °C was added 8.4 mmol of HX in 5 mL of toluene. The reactions were monitored by TLC, and upon completion of the reaction, the mixture was cooled to room temperature, filtered, and evaporated to dryness in vacuo and the product either chromatographed or recrystallized as described below.

$LMoO(NCS)_2$ was prepared by method 3 with NH_4NCS in DMF. The crude product was recrystallized from 1,2-dichloroethane–hexanes and obtained as red crystals. Anal. Calcd for $C_{17}H_{22}N_8OS_2BMo$: C, 38.86; H, 4.19; N, 21.33; S, 12.19. Found: C, 38.81; H, 4.22; N, 21.27; S, 12.11. IR: ν(MoO) 954 cm^{-1}.

$LMoO(N_3)_2$ was prepared by method 2 in DMF, dissolved in a minimum amount of 2:1 $C_2H_4Cl_2$–pentanes, and chromatographed on silica gel with the same solvent mixture. The product eluted as a bright orange band. Anal. Calcd for $C_{15}H_{22}N_{12}OBMo$: C, 36.52; H, 4.50; N, 34.08.

(8) Reynolds, M. S.; Berg, J. M.; Holm, R. H. *Inorg. Chem.* **1984**, *23*, 3057–3062.
(9) Berg, J. M.; Holm, R. H. *J. Am. Chem. Soc.* **1985**, *107*, 925–932.
(10) Kaul, B. B.; Enemark, J. H.; Merbs, S. L.; Spence, J. T. *J. Am. Chem. Soc.* **1985**, *107*, 2885–2891.
(11) Bray, R. C. *Adv. Enzymol. Relat. Areas Mol. Biol.* **1980**, *51*, 107–165.
(12) Trofimenko, S. *Chem. Rev.* **1972**, *72*, 497–509.
(13) Trofimenko, S. *Inorg. Chem.* **1971**, *10*, 504–507.
(14) Preliminary reports of portions of this work have been presented: (a) Enemark, J. H. Presented at the 188th National Meeting of the American Chemical Society, Philadelphia, PA, August 1984; paper INOR 6. (b) Enemark, J. H.; Cleland, W. E.; Collison, D.; Mabbs, F. E. *Rev. Port. Quim.* **1985**, *27*, 76–77. (c) Enemark, J. H.; Yamanouchi, K.; Barnhart, K.; Ortega, R.; Collison, D.; Mabbs, F. E. In *Some Recent Developments in the Chemistry of Chromium, Molybdenum and Tungsten: Proceedings of a Conference*; University of Sussex, July 1983; Dilworth, J., Lappert, M. F., Eds.; Royal Society of Chemistry, Dalton Division: London, England, 1983; poster 23. (d) Minelli, M.; Yamanouchi, K.; Enemark, J. H.; Subramanian, P.; Kaul, B. B.; Spence, J. T. *Inorg. Chem.* **1984**, *23*, 2554–2556.
(15) Trofimenko, S. *J. Am. Chem. Soc.* **1967**, *89*, 6288–6294.

Found: C, 36.30; H, 4.55; N, 33.28. IR: ν(MoO) 951 cm^{-1}; ν(N_3) 2068 cm^{-1}.

LMoO(OCH$_3$)$_2$ was prepared by method 2 and dissolved in a 1:1 mixture of dichloromethane–hexanes. Slow evaporation of the solution at aspirator pressure caused precipitation of a pale green solid, which was removed by filtration, identified as LMoOCl(OCH$_3$), and discarded. The filtrate was evaporated to dryness in vacuo and the above procedure repeated twice. The final light green product contained less than 1% LMoOCl(OCH$_3$) impurity. Anal. Calcd for $C_{17}H_{28}N_6O_3BMo$: C, 43.31; H, 5.94; N, 17.83. Found: C, 42.15; H, 5.68; N, 17.82. IR: ν(MoO) 931 cm^{-1}.

LMoO(OPh)$_2$ was prepared by method 2. Evaporation of the filtrate in vacuo to approximately half-volume resulted in separation of the product as red crystals, which were collected by filtration, washed with pentane, and air-dried. A second crop was obtained by concentration of the mother liquor in vacuo. Purification of the crude product was effected by dissolution in a minimum amount of benzene and chromatography on silica gel with benzene as eluant. Anal. Calcd for $C_{27}H_{32}N_6O_3BMo$: C, 54.45; H, 5.42; N, 14.11. Found: C, 54.40; H, 5.61; N, 14.06. IR: ν(MoO) 949 cm^{-1}.

LMoO(SEt)$_2$ was prepared by method 2, dissolved in benzene, and chromatographed on silica gel with benzene as eluant to give a green-brown powder. Anal. Calcd for $C_{19}H_{32}N_6OS_2BMo$: C, 42.92; H, 6.06; N, 15.81. Found: C, 43.22; H, 6.03; N, 15.73. IR: ν(MoO) 929 cm^{-1}.

LMoO(SPh)$_2$ was prepared by method 2, dissolved in a minimum amount of 2:1 dichloromethane–pentane, and chromatographed on silica gel to give dark green crystals. Anal. Calcd for $C_{27}H_{32}N_6OS_2BMo$: C, 51.67; H, 5.10; N, 13.40. Found: C, 51.40; H, 5.09; N, 13.26. IR: ν(MoO) 939 cm^{-1}.

LMoOCl(OCH$_3$) was prepared by method 1. The crude product was dissolved in a minimum amount of dichloromethane and chromatographed on silica gel with dichloromethane–pentanes (7:3) as eluant. The product was isolated as a green powder. Anal. Calcd for $C_{16}H_{25}N_6O_2BClMo$: C, 40.41; H, 5.30; N, 17.67; Cl, 7.45. Found: C, 40.52; H, 5.34; N, 17.60; Cl, 7.50. IR: ν(MoO) 947 cm^{-1}.

LMoOCl(OPh) was prepared by method 1, dissolved in a minimum amount of 1:1 dichloromethane–pentane, and chromatographed on silica gel. The product was obtained as purple microcrystals. Anal. Calcd for $C_{21}H_{27}N_6O_2ClBMo$: C, 46.90; H, 5.06; N, 15.63; Cl, 6.59. Found: C, 47.18; H, 5.17; N, 15.73; Cl, 6.65. IR: ν(MoO) 949 cm^{-1}.

LMoOCl(SEt) was prepared by method 2, dissolved in a minimum amount of benzene, and chromatographed on silica gel with benzene. A dark green band was eluted and the solvent evaporated to dryness in vacuo. The residue was dissolved in a minimum amount of 1:1 benzene–cyclohexane and chromatographed on silica gel with the same solvent mixture. The compound was obtained as dark green microcrystals. Anal. Calcd for $C_{17}H_{27}N_6OClSBMo$: C, 40.36; H, 5.38; N, 16.64. Found: C, 40.75; H, 5.38; N, 16.13. IR: ν(MoO) 945 cm^{-1}.

LMoOCl(SPh) was prepred by method 1, dissolved in a minimum amount of 1:1 dichloromethane–pentane, and chromatographed on silica gel to give green crystals. Anal. Calcd for $C_{21}H_{27}N_6OClSBMo$: C, 45.53; H, 4.88; N, 15.18. Found: C, 45.50; H, 4.94; N, 15.55. IR: ν(MoO) 943 cm^{-1}.

LMoO(1-O,O) was prepared by method 1; the crude product was dissolved in toluene and the solution filtered to remove Et_3NHCl. Evaporation of the filtrate gave a blue powder. Anal. Calcd for $C_{17}H_{26}N_6O_3BMo$: C, 43.50; H, 5.54; N, 17.91. Found: C, 43.48; H, 5.60; N, 17.86. IR: ν(MoO) 938 cm^{-1}.

LMoO(1-O,S) was prepared by method 1, dissolved in a minimum amount of benzene, and chromatographed on silica gel to give a bright green powder. Anal. Calcd for $C_{17}H_{26}N_6O_2SBMo$: C, 42.06; H, 5.36; N, 17.32. Found: C, 41.81; H, 5.36; N, 17.52. IR: ν(MoO) 928 cm^{-1}.

LMoO(1-S,S) was prepared by method 2, dissolved in a minimum amount of benzene, and chromatographed on silica gel to give a dark green-brown powder. Anal. Calcd for $C_{17}H_{26}N_6OS_2BMo$: C, 40.74; H, 5.23; N, 16.77; S, 12.77. Found: C, 39.26; H, 5.04; N, 15.64; S, 14.93. IR: ν(MoO) 927 cm^{-1}.

LMoO(2-O,O) was prepared by method 2, dissolved in a minimum amount of benzene, and chromatographed on silica gel with benzene. The product eluted as a dark green-brown band. Anal. Calcd for $C_{21}H_{26}N_6O_3BMo$: C, 48.74; H, 5.03; N, 16.25. Found: C, 48.78; H, 5.14; N, 16.21. IR: ν(MoO) 940 cm^{-1}.

LMoO(2-O,NH) was prepared by method 1 and dissolved in a minimum amount of 1,2-dichloroethane. The product eluted as a dark brown band. Anal. Calcd for $C_{21}H_{27}N_7O_2BMo$: C, 48.83; H, 5.23; N, 18.99. Found: C, 48.60; H, 5.57; N, 18.72. IR: ν(MoO) 916 cm^{-1}.

LMoO(2-O,S) was prepared by method 1, dissolved in a minimum amount of benzene, and chromatographed on silica gel with benzene. The product eluted as a dark brown band. Anal. Calcd for $C_{21}H_{26}N_6O_2SBMo$: C, 47.30; H, 4.88; N, 15.76. Found: C, 47.15; H, 5.00; N, 14.45. IR: ν(MoO) 936 cm^{-1}.

LMoO(2-S,S) was prepared from toluenedithiol by method 1, dissolved in a minimum amount of benzene, and chromatographed on silica gel with benzene. The product eluted as a dark green-brown band. Anal. Calcd for $C_{22}H_{28}N_6OS_2BMo$: C, 46.90; H, 4.97; N, 14.92. Found: C, 47.90; H, 4.86; N, 14.44. IR: ν(MoO) 925 cm^{-1}.

LMoO(2-S,NH) was prepared by method 3 and dissolved in a minimum amount of 1,2-dichloroethane. The product was eluted as a dark brown band. Anal. Calcd for $C_{21}H_{27}N_7OSBMo$: C, 47.36; H, 5.08; N, 18.42. Found: C, 47.08; H, 5.24; N, 17.89. IR: ν(MoO) 910 cm^{-1}.

Physical Measurements. Infrared spectra were obtained in KBr pellets on a Perkin-Elmer PE983 spectrometer. Optical spectra were obtained on either a IBM 9420 or a Varian 2390 spectrophotometer. Mass spectra were obtained with an AEI MS30 mass spectrometer with ionization effected by electron impact. Electron paramagnetic resonance (EPR) spectra as either fluid solutions or frozen glasses in toluene were obtained at X-band frequencies with a Varian E112 spectrometer equipped with an Oxford Instruments ESR9 continuous-flow cryostat. Cyclic voltammetric measurements were performed on acetonitrile or DMF solutions (~1 mM) over the potential range +1.5 to −2.0 V (vs. Ag/AgCl) at a platinum-disk electrode on an IBM EC 225 voltammetric analyzer equipped with an IBM 742MT X-Y-T recorder.

X-ray Structure Determination of LMoO(SPh)$_2$. Dark green crystals of LMoO(SPh)$_2$ were obtained by preparative method 2. The determination of the Bravais lattice and cell dimensions and the collection of the intensity data were carried out on a Nicolet-Syntex $P2_1$ diffractometer equipped with a graphite monochromator. The cell constants were determined from a least-squares refinement based on 22 reflections having $15° < 2\theta < 20°$. The crystal system and axial lengths were confirmed by axial photographs. Several ω scans showed widths at half-height of 0.45°, indicating moderate crystal quality. The diffraction conditions $h0l$, $l = 2n$, and $0k0$, $k = 2n$, uniquely determine the space group as $P2_1/c$. Data were corrected for Lorentz and polarization effects, but no corrections were made for absorption or extinction. The structure was solved by direct methods and refined by full-matrix least-squares techniques.[16] Hydrogen atoms were included as fixed contributions in idealized positions. Anomalous dispersion corrections were included for all non-hydrogen atoms. Table I summarizes the crystal and refinement

Table I. Summary of the Crystal and Refinement Data for LMoO(SPh)$_2$

formula	$C_{27}H_{32}MoBN_6OS_2$
mol wt	627.47
color, shape	green, square prism
space group	$P2_1/c$
a, Å	13.079 (6)
b, Å	14.438 (7)
c, Å	15.836 (9)
β, deg	104.73 (4)
V, Å^3	2892.1
temp, °C	23 (1)
Z	4
d_{calcd}, g/cm^3	1.44
radiation, Å	Mo Kα (λ = 0.71073)
μ, cm^{-1}	6.1
cryst dimens, mm	0.13 × 0.15 × 0.66
cryst–detector dist, cm	21
scan speed, deg/min	variable, 3–15
scan type	θ–2θ
scan width, deg	$2\theta(K\alpha_1)$ − 1.0 to $2\theta(K\alpha_2)$ + 1.0
peak bkgd counting time	2:1
maximum 2θ, deg	50
no. of reflecns measd	4279 total, 3650 unique
agreement for equiv reflecns	2.8%
no. of unique data used (NO)	2813 with $\|F_o\| > \sigma\|F_o\|$
function minimized	$\sum w(\|F_o\| - \|F_c\|)^2$
least-squares wts (w)	$4F_o^2/\{\sigma^2(F_o^2) + (cF_o^2)^2\}$, c = 0.03
parameters refined (NV)	343
$R_1 = \sum(\|F_o\| - \|F_c\|)/\sum\|F_o\|$	0.071
$R_2 = \{\sum w(\|F_o\| - \|F_c\|)^2/\sum wF_o^2\}^{1/2}$	0.055
GOF = $\{\sum w(\|F_o\| - \|F_c\|)^2/(NO - NV)\}^{1/2}$	1.6
max residual electron density, e/Å^3	0.96 (11)

(16) All computations were carried out on a PDP 11/34a computer using the Structure Determination Package (SDP) of B. A. Frenz & Associates, Inc., College Station, TX, and Enraf-Nonius, Delft, Holland.

Table II. Positional Parameters and Their Estimated Standard Deviations[a]

atom	x	y	z	B_{eq}, Å^2
Mo	0.22452 (5)	0.17564 (5)	0.06022 (5)	3.91 (1)
S1	0.3659 (2)	0.1257 (2)	0.1784 (2)	4.99 (6)
S2	0.0977 (2)	0.1158 (2)	0.1303 (2)	5.48 (6)
O	0.2329 (4)	0.4088 (3)	0.4895 (4)	5.4 (2)
N11	0.2254 (4)	0.3127 (4)	0.1413 (4)	3.8 (1)
N12	0.2269 (4)	0.3957 (4)	0.0999 (4)	3.6 (1)
N21	0.1075 (4)	0.2540 (4)	0.9661 (4)	3.7 (2)
N22	0.1202 (4)	0.3474 (4)	0.9525 (4)	3.5 (1)
N31	0.3394 (4)	0.2598 (4)	0.0126 (4)	3.8 (2)
N32	0.3176 (4)	0.3500 (4)	-0.0123 (4)	3.7 (1)
C11	0.2306 (5)	0.3322 (6)	0.2256 (5)	4.3 (2)
C12	0.2366 (6)	0.4275 (6)	0.2363 (5)	4.8 (2)
C13	0.2351 (5)	0.4635 (5)	0.1567 (5)	4.2 (2)
C14	0.2282 (7)	0.2631 (7)	0.2920 (6)	5.9 (3)
C15	0.2449 (7)	0.5637 (6)	0.1346 (6)	6.4 (3)
C21	0.9760 (6)	0.7278 (5)	0.5958 (5)	4.1 (2)
C22	0.0188 (6)	0.7002 (5)	0.1488 (5)	4.7 (2)
C23	0.0443 (6)	0.3731 (5)	0.8815 (5)	4.3 (2)
C24	0.0109 (6)	0.6286 (6)	0.6062 (7)	6.3 (3)
C25	0.0365 (7)	0.4704 (6)	-0.1516 (6)	6.4 (3)
C31	0.4293 (6)	0.2631 (5)	0.4908 (5)	4.4 (2)
C32	0.4630 (6)	0.3122 (6)	0.9534 (5)	5.2 (2)
C33	0.3926 (6)	0.3810 (5)	0.9498 (5)	4.4 (2)
C34	0.4748 (6)	0.3575 (6)	0.5018 (7)	6.7 (3)
C35	0.3886 (7)	0.4766 (6)	0.9143 (6)	6.2 (2)
C41	0.3781 (6)	0.4968 (5)	0.6840 (5)	4.4 (2)
C42	0.4739 (6)	0.5328 (6)	0.7274 (6)	5.2 (2)
C43	0.4859 (7)	0.6269 (6)	0.7412 (7)	6.7 (3)
C44	0.4050 (7)	0.6848 (6)	0.7099 (7)	7.1 (3)
C45	0.3110 (7)	0.6522 (6)	0.6640 (8)	8.1 (3)
C46	0.2972 (6)	-0.0572 (6)	0.1514 (7)	7.4 (3)
C51	0.9716 (5)	0.3304 (6)	0.6070 (5)	4.4 (2)
C52	-0.1144 (6)	0.1126 (6)	0.0957 (8)	7.3 (3)
C53	-0.2130 (7)	0.1463 (6)	0.0878 (8)	8.6 (3)
C54	-0.2282 (6)	0.2401 (6)	0.0897 (7)	7.4 (3)
C55	0.1448 (7)	0.7036 (5)	0.9013 (7)	7.1 (3)
C56	0.0454 (6)	0.7376 (5)	0.8910 (6)	5.9 (3)
B	0.2194 (7)	0.3964 (6)	0.0026 (7)	4.2 (2)

[a] Anisotropically refined atoms are given in the form of the isotropic equivalent thermal parameter defined as $8\pi^2(U_{11} + U_{22} + U_{33})/3$.

data. Final atomic parameters appear in Table II. Anisotropic thermal parameters, idealized hydrogen atom parameters, and calculated structure factors are available in the supplementary material.

Results and Discussion

Synthesis. An extensive series of LMoOXY complexes can be prepared by several routes from the common precursor $LMoOCl_2$, first reported by Trofimenko[13] as a product of the reaction of $[LMo(CO)_3]^-$ with $SOCl_2$. We have developed a more convenient preparation for $LMoOCl_2$. Reaction of $MoCl_5$ with THF under anaerobic conditions (eq 1) yields the known $MoOCl_3(THF)_2$,

$$MoCl_5 \xrightarrow{THF} MoOCl_3(THF)_2 \xrightarrow{KL} LMoOCl_2 \quad (1)$$

presumably by abstraction of an oxygen atom from the solvent. Addition of KL to the reaction mixture and moderate heating affords $LMoOCl_2$ as a green precipitate, which can be recrystallized from hot dichloromethane or 1,2-dichloroethane as bright green crystals. Typical yields are 50–70%. The complex is stable in air indefinitely, is stable to water, and is unchanged at 200 °C.

All other LMoOXY complexes can be prepared from $LMoOCl_2$ by one or more methods. In reaction 2, chloride substitution on

$$LMoOCl_2 + HX + Et_3N \rightarrow LMoOClX + Et_3NHCl \quad (2)$$

$$LMoOCl_2 + 2NaX \rightarrow LMoOX_2 + 2NaCl \quad (3)$$

$LMoOCl_2$ is effected by reaction with the appropriate alcohol or thiol and an equimolar amount of triethylamine in a nonpolar solvent such as toluene at elevated temperature. Substitution reaction 3 involves addition of the sodium salt of the appropriate thiol or alcohol to a slurry of $LMoOCl_2$ at elevated temperature. Both mono- and disubstituted complexes can be prepared by (2) and (3) by appropriate choice of reagent stoichiometries.

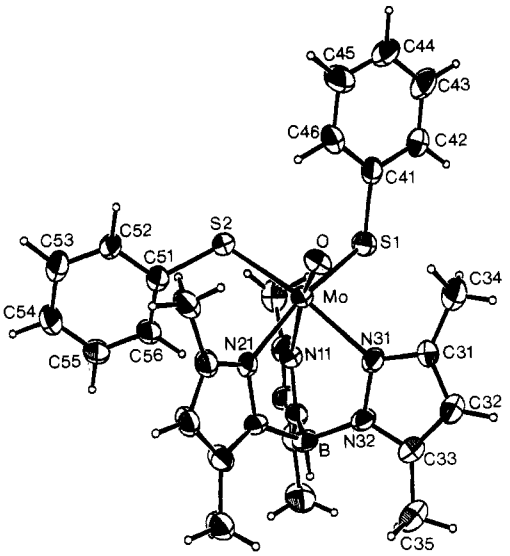

Figure 2. Perspective view of the structure of $LMoO(SPh)_2$. The atoms are drawn as 33% probability ellipsoids.

The elevated reaction temperatures necessary to obtain ligand substitution by (2) and (3) can result in complicating side reactions depending on the nature of the incoming ligand. These side reactions are presumed to be dimerization, as indicated by an intense optical absorption band at ~460 nm,[17] and reduction. Reaction 4 provides a convenient route to disubstituted complexes

$$LMoO(1\text{-}O,O) + 2NH_4NCS \rightarrow LMoO(NCS)_2 + HOCH_2CH_2OH + 2NH_3 \quad (4)$$

provided that the reactant bears protons more acidic than those of ethylene glycol. This condition is satisfied by aromatic reactants, e.g. catechol and mercaptophenol, and by ammonium salts of anionic ligands. Unlike $LMoOCl_2$, the LMoOXY complexes prepared by reactions 2–4 are not stable in air indefinitely and are stored under nitrogen.

There is no evidence for ligand substitution reactions of $LMoOCl_2$ at room temperature. Few detailed studies of ligand substitution reactions in oxo–Mo(V) complexes have appeared, but Garner and co-workers[18] have investigated the kinetics of the ligand-exchange reactions of $MoOCl_3(OPPh_3)_2$. Their results indicated that ligand exchange occurs by dissociation of the ligand trans to the oxo group followed by coordination of the new ligand. In the present case, this trans site is occupied by a pyrazole nitrogen atom of L. In addition, the sterically crowded pocket provided by L makes an associative substitution pathway unlikely. Therefore, ligand-exchange reactions of $LMoOCl_2$ probably proceed by dissociation of chloride and subsequent coordination of the new ligand.

Structure of $LMoO(SPh)_2$. The structure of $LMoO(SPh)_2$, determined by single-crystal X-ray diffraction, is shown in Figure 2. The terminal oxo group and the two thiolate ligands are constrained to be mutually cis to one another by the *fac* stereochemistry imposed by L. The two Mo–S distances (Table III) are indistinguishable (2.382 (2) Å average) and slightly shorter than the average Mo–S distance in a six-coordinate oxomolybdenum(V) complex[19] in which the two thiolate ligands are trans to one another (2.409 (7) Å). In the five-coordinate oxo-

(17) Lincoln, S. Ph.D. Dissertation, State University of New York at Stony Brook, 1982.
(18) (a) Garner, C. D.; Hyde, M. R.; Mabbs, F. E.; Routledge, V. I. *J. Chem. Soc., Dalton Trans.* **1975**, 1175–1180. (b) Garner, C. D.; Hyde, M. R.; Mabbs, F. E.; Routledge, V. I. *J. Chem. Soc., Dalton Trans.* **1975**, 1180–1186. (c) Hyde, M. R.; Garner, C. D. *J. Chem. Soc., Dalton Trans.* **1975**, 1186–1191. (d) Garner, C. D.; Hyde, M. R.; Mabbs, F. E. *Nature (London)* **1975**, *253*, 623–625. (e) Garner, C. D.; Hyde, M. R.; Mabbs, F. E.; Routledge, V. I. *J. Chem. Soc., Dalton Trans.* **1977**, 1198–1201.
(19) Yamonouchi, K.; Enemark, J. H. *Inorg. Chem.* **1979**, *18*, 1626–1633.

Table III. Bond Distances and Angles in $LMoO(SPh)_2$

atom 1	atom 2	dist, Å	atom 1	atom 2	dist, Å
Mo	S1	2.383 (2)	Mo	N21	2.164 (5)
Mo	S2	2.380 (2)	Mo	N31	2.207 (5)
Mo	O	1.676 (4)	Mo	C41	1.777 (7)
Mo	N11	2.357 (5)	Mo	C51	1.775 (6)

atom 1	atom 2	atom 3	angle, deg
S1	Mo	S2	90.98 (7)
S1	Mo	O	97.8 (2)
S1	Mo	N11	86.1 (1)
S1	Mo	N21	166.1 (1)
S1	Mo	N31	86.6 (1)
S2	Mo	O	102.7 (2)
S2	Mo	N11	87.6 (1)
S2	Mo	N21	93.3 (1)
S2	Mo	N31	166.9 (1)
O	Mo	N11	168.9 (2)
O	Mo	N21	94.2 (2)
O	Mo	N31	90.3 (2)
N11	Mo	N21	80.9 (2)
N11	Mo	N31	79.3 (2)
N21	Mo	N31	84.3 (2)
Mo	S2	C41	112.5 (3)
Mo	S1	C51	117.7 (2)

molybdenum(V) complex $[MoO(SPh)_4]^-$, the average Mo–S distance is 2.403 (5) Å.[20] The Mo–S distances obtained from EXAFS studies of sulfite oxidase are in the range 2.42–2.38 Å.[6] The S1···S2 distance of 3.4 Å is a normal nonbonded contact. This is in contrast to the short S···S distances of ~2.75 Å observed for certain dioxomolybdenum(VI) complexes.[21]

The bond angles about the molybdenum atom deviate significantly from octahedral geometry. The effective coordination symmetry is only C_1, as illustrated by S1–Mo–O = 97.7 (2)° and S2–Mo–O = 102.7 (2)°. The environments of the two thiolate ligands of $LMoO(SPh)_2$ are also distinctly different in the solid state. The thiolate ligand containing S1 is oriented so that its phenyl group projects into the pocket formed by the protecting methyl groups of L and is characterized by a C–S1–Mo–O torsional angle of −34°. The thiolate ligand containing S2 has its phenyl group lying between two pyrazole rings of L and has a C–S2–Mo–O torsional angle of −110°. The EPR data for $LMoO(SPh)_2$ suggest that the thiolates remain inequivalent in frozen solution (vide infra).

The thiolate torsion angles and the associated inequalities in S–Mo–O angles for $LMoO(SPh)_2$ are similar to the distorted coordination geometry previously described for $MoOCl(tox)_2$ (tox is 8-mercaptoquinolinate).[19] The distortions in $MoOCl(tox)_2$ were explained on the basis of repulsions between filled sulfur orbitals and the π-electron density in the short Mo=O bond. Such repulsions are greater for structure III than for structure II. For

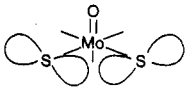

II

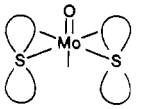

III

$LMoO(SPh)_2$, the C–S1–Mo–O torsion angle is within 34° of geometry II and the C–S2–Mo–O torsion angle is within 20° of geometry III. Thus, the larger S2–Mo–O angle in $LMoO(SPh)_2$ can be explained by nonbonded repulsions between the filled pπ orbital on sulfur and π-electron density in the Mo=O bond. The two different thiolate orientations also lead to unequal Mo–N distances trans to the S atoms (Mo–N21 = 2.164 (5) Å and Mo–N31 = 2.207 (5) Å). The relatively long Mo–N31 distance[22] is a further reflection of the repulsions between S2 and O, which in turn make the O–Mo–N31 angle 4° smaller than the O–Mo–N21 angle. The substantially longer Mo–N11 distance (2.357 (5) Å) is expected for an atom trans to an oxo group.

The dimensions of the hydrotris(3,5-dimethyl-1-pyrazolyl)borate ligand are similar to those found in other studies.[22] It is interesting to note that the rotational conformations of the thiolate ligands result in their sulfur pπ orbitals being approximately in the same orientation as the pπ orbitals of their respective trans pyrazole rings. This latter observation suggests that the polypyrazolylborate ligand and the terminal oxo group both play major roles in the molecular and electronic structures of LMoOXY compounds.

Table IV. Electron Paramagnetic Resonance Data[a]

compd	g_1	g_2	g_3	$\langle g \rangle^b$	$\langle A \rangle^c$
$LMoOCl_2$ (**1**)	1.967	1.941	1.929	1.947	46.0
$LMoO(NCS)_2$ (**2**)	1.954	1.944	1.933	1.943	42.9
$LMoO(N_3)_2$ (**3**)	1.967	1.937	1.927	1.944	44.4
$LMoO(OMe)_2$ (**4**)	1.960	1.942	1.904	1.937	45.2
$LMoO(OPh)_2$ (**5**)	1.959	1.938	1.901	1.932	44.2
$LMoO(SEt)_2$ (**6**)	2.011	1.952	1.931	1.966	36.7
$LMoO(SPh)_2$ (**7**)	2.004	1.950	1.937	1.967	35.8
LMoO(Cl,OMe) (**8**)	1.967	1.943	1.903	1.939	46.2
LMoO(Cl,OPh) (**9**)	1.964	1.942	1.912	1.940	46.2
LMoO(Cl,SEt) (**10**)	1.996	1.948	1.922	1.957	41.1
LMoO(Cl,SPh) (**11**)	1.992	1.947	1.922	1.955	41.3
LMoO(1-O,O) (**12**)	1.974	1.963	1.908	1.949	37.8
LMoO(1-O,S) (**13**)	1.991	1.965	1.932	1.961	38.0
LMoO(1-S,S) (**14**)	2.016	1.971	1.942	1.976	35.9
LMoO(2-O,O) (**15**)	1.970	1.968	1.925	1.953	38.4
LMoO(2-O,NH)[d] (**16**)	1.971	1.964	1.928	1.955	39.2
LMoO(2-O,S) (**17**)	1.979	1.965	1.932	1.960	38.3
LMoO(2-S,S)[e] (**18**)	2.004	1.974	1.937	1.972	34.3
LMoO(2-S,NH)[d] (**19**)	1.993	1.973	1.926	1.964	38.1
trans-$MoOCl_3$(phen)[f]	1.971	1.941	1.929	1.947	46.6
trans-MoOCl{$(sal)_2$phen}[f]	1.955	1.947	1.926	1.940	44.1
$[MoO(mae)]^-$[g]	2.002	1.982	1.974	1.986	33.0
$[MoO(mab)]^-$[g]	2.004	1.979	1.973	1.986	33.0
$[MoOCl_4]^-$[h]	1.967	1.950		1.956	47.9
$[MoO(NCS)_5]^{2-}$[i]	1.928	1.944		1.935	50.0
$[MoO(SPh)_4]^-$[j]	2.017	1.979		1.990	32.3

[a] X-Band frequencies, in toluene at 77 K. Estimated errors on g values are ±0.002 and on $\langle A \rangle$ are $\pm 0.5 \times 10^{-4}$ cm^{-1}. [b] Measured at 296 K. [c] ^{95,97}Mo, $\times 10^{-4}$ cm^{-1}. [d] $\langle A \rangle_{1H} = 8.2 \times 10^{-4}$ cm^{-1} for **16** and 8.3×10^{-4} cm^{-1} for **19**. [e] 2-S, S = toluenedithiolate. [f] Data from ref 23a. phen is *o*-phenanthroline; $(sal)_2$phen is disalicylaldehyde *o*-phenylenediimine. [g] Data from ref 23b. $maeH_4$ is 1,2-bis(2-mercaptoanilino)ethane; $mabH_4$ is 2,3-bis(2-mercaptoanilino)butane. [h] Data from ref 24. [i] Data from ref 25. [j] Data from ref 26.

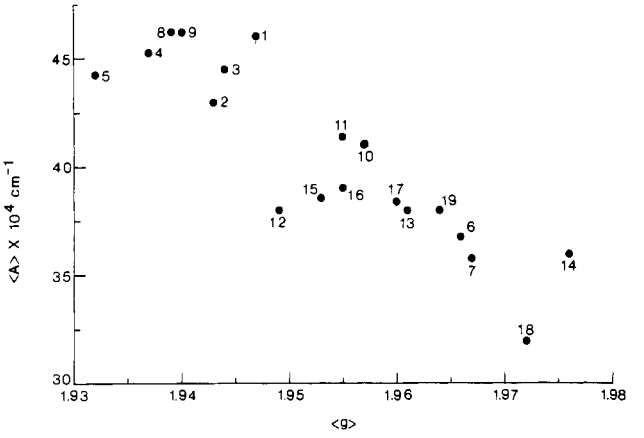

Figure 3. Correlation of $\langle g \rangle$ and $\langle A \rangle$(^{95,97}Mo) for LMoOXY compounds. See Table IV for the identities of individual compounds.

EPR Spectra. The isotropic and anisotropic g values and the isotropic ^{95,97}Mo hyperfine parameter, $\langle A \rangle$, for each complex appear in Table IV. The EPR spectra for the complexes in fluid

(20) Bradbury, J. R.; Mackay, M. F.; Wedd, A. G. *Aust. J. Chem.* **1978**, *31*, 2423–2430.

(21) (a) Berg, J. M.; Spira, D. J.; Hodgson, K. O.; Bruce, A. E.; Miller, K. F.; Corbin, J. L.; Stiefel, E. I. *Inorg. Chem.* **1984**, *23*, 2412–2418. (b) Stiefel, E. I.; Miller, K. F.; Bruce, A. E.; Heinecke, J.; Pariyadath, N.; Corbin, J.; Berg, J. M.; Hodgson, K. O. In *Molybdenum Chemistry of Biological Significance*; Newton, W. E., Otsuka, S., Eds.; Plenum: New York, 1980; pp 279–294.

(22) Lincoln, S.; Soong, S.-L.; Koch, S. A.; Sato, M.; Enemark, J. H. *Inorg. Chem.* **1985**, *24*, 1355–1359.

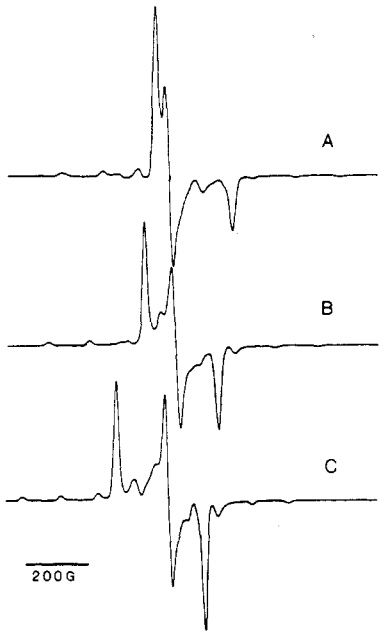

Figure 4. Comparison of the EPR spectra for LMo(1-X,Y) complexes as O is replaced by S: (A) LMoO(1-O,O); (B) LMoO(1-O,S); (C) LMoO(1-S,S). Spectra are at X-band, obtained at 77 K in frozen toluene solution.

and frozen toluene solutions indicate that for each compound only one EPR-active molybdenum species is present. The kinetic inertness of the complexes and the poor ligating ability of the solvent ensure that the values of the table are the molecular parameters of the listed compounds.

The isotropic spin-Hamiltonian parameters $\langle g \rangle$ and $\langle A \rangle$ are correlated graphically in Figure 3. As expected, an inverse correlation of $\langle A \rangle$ with $\langle g \rangle$ is found and a "clustering" of compounds occurs according to the nature of the donor atoms X,Y, which are in the plane perpendicular to the terminal oxo group. This behavior contrasts with that observed by Scullane et al.,[23] where no domains for ligand type were identified. However, the ligands of the earlier study[23] did not constrain the molybdenum atom to a common coordination geometry as occurs for the LMoOXY compounds reported here. In the LMoOXY compounds the presence of at least one sulfur donor atom generally results in a large $\langle g \rangle$ being associated with a small value of $\langle A \rangle$, whereas oxygen donors give rise to smaller values of $\langle g \rangle$ associated with larger $\langle A \rangle$ parameters. All of the compounds studied here have a pair of nitrogen atoms cis to the terminal oxo group.

Table IV also includes EPR parameters for several other oxo–Mo(V) compounds. The reported EPR parameters for *trans*-$MoOCl_3$(phen) (where the probable equatorial ligands are N_2Cl_2) are similar to those for $LMoOCl_2$, and the parameters[23a] for *trans*-MoOCl{(sal)$_2$phen} (probable N_2O_2 equatorial ligands) are similar to those for $LMoO(OMe)_2$. The close similarity between the EPR parameters within each pair suggests that the EPR parameters of the present LMoOXY complexes may generally be compared to those of other oxomolybdenum(V) complexes with similar sets of donor ligands. The EPR parameters for [MoO(mae)]$^-$ and [MoO(mab)]$^-$, complexes of tetradentate N_2S_2 ligands,[23b] are similar to those for LMoO(1-S,S) and LMoO(2-S,S), although the latter pair have smaller g_3 values.

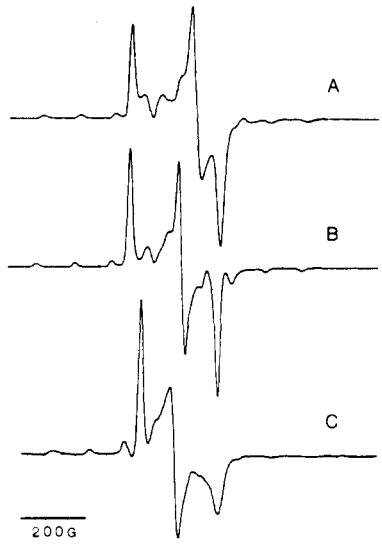

Figure 5. Comparison of the frozen-solution EPR spectra for LMoO(SR)$_2$ complexes possessing different SR ligands: (A) $LMoO(SEt)_2$; (B) LMoO(1-S,S); (C) LMoO(2-S,S). Spectra are at X-band, obtained at 77 K in frozen toluene.

Comparison of the EPR data for $LMoOX_2$ complexes with data for high-symmetry $[MoOX_4]^-$ and $[MoOX_5]^{2-}$ systems (Table IV) shows that the trend of $\langle g \rangle$ (NCS < Cl < SPh) is mirrored by $LMoO(NCS)_2$, $LMoOCl_2$, and $LMo(SPh)_2$. For both sets of complexes $\langle A \rangle$ is smallest when X = SPh.

The point symmetry at the molybdenum atom of the LMoOXY complexes can be no higher than C_s, and complete anisotropy in the principal components of the **g** tensor is permitted. The values of g_i in Table IV were obtained by direct measurement from the *frozen*-solution EPR spectra. In all cases $\sum g_i/3$ is in good agreement with $\langle g \rangle$ obtained directly from *fluid*-solution measurements at room temperature. The inclusion of at least one sulfur atom in the donor set produces one g_i value greater than 1.975, and where X = Y = S one value of g_i is always greater than 2.0023. In contrast, when X = Y = O or when X = O, Y = Cl, there is always a value of $g_i \leq 1.912$. Figure 4 illustrates the increase in g_1 and in the difference between g_1 and g_2 as oxygen is replaced by sulfur for the series LMoO(1-O,O), LMoO(1-O,S), and LMoO(1-S,S). Similar behavior is also observed for the series LMoO(2-O,O), LMoO(2-O,S), and LMoO(2-S,S).

From the data in Table IV it appears that there is a chelate effect on the anisotropy in the g values when comparing compounds for which X = Y. For the compounds $LMoO(OMe)_2$, LMoO(1-O,O), and LMoO(2-O,O), the separation between g_1 and g_2 becomes smaller across the series while g_3 is nearly constant. A similar effect is observed for the series $LMoO(SEt)_2$, LMoO(1-S,S), and LMoO(2-S,S), although the decrease in the separation between g_1 and g_2 is less marked (Figure 5). The observed variations in g for the thiolate series could arise from slight differences in the S–Mo–S bond angles for the complexes. However, the rotational orientations of the SR ligands are also likely to be important in determining the individual g values. The bidentate 1-S,S and 2-S,S ligands require that the filled 3p orbitals on both sulfur atoms be approximately parallel to the Mo=O bond (III), whereas monodentate thiolate ligands can adopt several conformations relative to the Mo=O group. The mixing of the filled sulfur 3p orbitals with the Mo 4d orbitals will depend upon the rotational conformation of the thiolate ligand. The importance of the rotational conformations of thiolate ligands on the structure and reactivity of $(\eta^5\text{-}C_5H_5)Mo(NO)(SR)_2$ has recently been demonstrated.[27]

The foregoing discussion, together with that in the Introduction, provide a basis for comparison between the EPR parameters of the LMoOXY compounds and those of the EPR-active Mo(V) states of oxo–molybdoenzyme preparations. One current view

(23) (a) Scullane, M. I.; Taylor, R. D.; Minelli, M.; Spence, J. T.; Yamanouchi, K.; Enemark, J. E.; Chasteen, N. D. *Inorg. Chem.* **1979**, *18*, 3213–3219. (b) Rajan, O. A.; Spence, J. T.; Leman, C.; Minelli, M.; Enemark, J. H.; Kroneck, P. M. H.; Sulger, K. *Inorg. Chem.* **1983**, *22*, 3065–3072.

(24) Garner, C. D.; Hill, L. H.; Mabbs, F. E.; McFadden, D. L.; McPhail, A. T. *J. Chem. Soc., Dalton Trans.* **1977**, 853–858.

(25) Galub, A. M.; Grechiklrina, V. A.; Trachevskii, V. V.; Ui'ko, N. V. *Zh. Neorg. Khim.* **1979**, *18*, 1120.

(26) Hanson, G. R.; Brunette, A. G.; McDonell, A. C.; Murray, K. S.; Wedd, A. G. *J. Am. Chem. Soc.* **1981**, *103*, 1953–1959.

(27) Ashby, M. T.; Enemark, J. H. *J. Am. Chem. Soc.* **1986**, *108*, 730–733.

Table V. EPR Data from Molybdenum Cofactor Solutions[a]

cofactor soln	g_1	g_2	g_3	$\langle g \rangle$
form 1	2.029	1.978	1.978	1.995
form 2	1.978	1.959	1.941	1.959
form 1 + PhSH	2.026	1.979	1.979	1.995
form 1 + $HSCH_2CH_2SH$	2.044	1.983	1.979	2.002
form 1 + $HSCH_2CH_2OH$	2.008	1.977	1.969	1.984

[a] Reproduced from ref 29.

of the molybdenum centers in such enzymes involves cis coordination by two sulfur atoms of the side chain of the molybdopterin ring of the molybdenum cofactor (I).[4] Additional ligation by the pendant phosphate group or by atoms of the pterin ring system may also occur. The molybdenum atom in the cofactor will also have at least one terminal oxo group, which almost certainly is cis to the two sulfur atoms.

To a first approximation, the stereochemical constraints of the LMoOXY compounds model the proposed stereochemistry of the molybdenum cofactor. Four different complexes, $LMoO(SEt)_2$, $LMo(SPh)_2$, LMoO(1-S,S), and LMoO(2-S,S), contain SR groups in a cis stereochemistry as required by structure I,[4] and LMoO(2-S,S) possesses the postulated dithiolene-type carbon skeleton of the chelate ligand. The variations in the g values among these $LMoO(SR)_2$ complexes (Table IV, Figure 5) were discussed above. Comparison of the g values with EPR data tabulated[2,7,11] for "oxo-type" molybdoenzymes reveals that in general the model compounds have smaller g_3 values than the enzyme preparations. No model compound exactly matches the EPR parameters of an enzyme. The g values for LMoO(2-S,S) most closely resemble the low-pH signal of sulfite oxidase (g_1 = 2.003, g_2 = 1.972, g_3 = 1.965, $\langle g \rangle$ = 1.980),[28a] whereas the g values for $LMoO(SEt)_2$ are more similar to the very rapid signal of xanthine oxidase (g_1 = 2.025, g_2 = 1.955, g_3 = 1.949, $\langle g \rangle$ = 1.976).[28c]

In a recent study Hawkes and Bray[29] investigated the EPR parameters for molybdenum cofactor solutions prepared from denatured bovine xanthine oxidase under anaerobic and reducing conditions. The observed EPR parameters were assigned to $[MoO]^{3+}$ moieties derived from two forms of the cofactor. The trends in g values for thiol-treated cofactor solutions (Table V) parallel the changes induced by the addition of thiolates to LMoOXY compounds, but the magnitudes of the changes in g values are greater for the model compounds than for the cofactor preparations. This result is consistent with the difference in their respective starting coordination fragments. The models contain the $\{MoON_3\}$ unit, whereas the cofactor is thought to contain an $\{MoOS_2\}$ unit. These qualitative observations support the structural hypothesis of coordination of the added thiol ligand cis to a terminal oxo group in the cofactor. However, the data of Table IV and the previous discussion also demonstrate that the EPR spectra of discrete $[MoO]^{3+}$ centers are extremely sensitive to changes in the donor atoms and in the geometrical constraints of the coordinated ligands (Figure 5, for example). Therefore, caution is advised in associating specific structures with the EPR spectral changes observed for cofactor solutions.

The X-band fluid-solution EPR spectra of LMoO(2-O,NH) and LMoO(2-S,NH) are of particular interest (Figure 6). We ascribe the splittings of the molybdenum $I = 0$ and $I = {}^5/_2$ lines in these spectra to the interaction with the single proton on the nitrogen atom of the 2-S,NH and 2-O,NH ligands.[30] This assignment was confirmed by treating toluene solutions of the compounds with D_2O (99.8%), which removed the splittings. The original spectra could be regenerated by shaking the D_2O-treated solutions with H_2O. Treatment of a fresh toluene solution of either

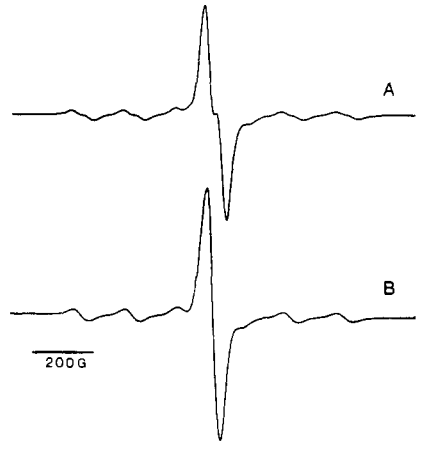

Figure 6. Proton splitting of the EPR spectrum of LMoO(2-S,NH): (A) original spectrum; (B) spectrum after addition of D_2O. Spectra are at X-band, obtained at 22 °C in toluene.

LMoO(2-O,NH) or LMoO(2-S,NH) with H_2O did not affect the EPR spectra. The isotropic proton splitting (9 G) was determined from simulations and is comparable to the line width in both compounds. The EPR spectra of frozen solutions of these two compounds at 77 K were not sufficiently well-resolved to enable the expected anisotropy in the proton hyperfine splitting to be measured.[31] The proton splitting of 9 G observed for these complexes is comparable to the average proton splitting observed in the EPR spectra of several oxomolybdenum enzymes; 9.8 G for the low-pH form of sulfite oxidase,[28] 9.2 for the low-pH form of nitrate reductase,[28b] and 10.1 for the rapid type 2 signal of xanthine oxidase.[28c]

The low symmetry of the molybdenum center of the LMoOXY compounds (C_s or C_1, vide supra) means that the three principal axes of the **A** tensor are not all required to be coincident with those of the **g** tensor. In C_s symmetry only one coincidence is required; in C_1 none are required. In addition, the usual assumption that the oxo ligand dominates the electronic structure of oxo–Mo(V) centers may not be valid for LMoOXY compounds, which also possess a strong trigonal field from L (Figure 1). This paper restricts the discussion of the molybdenum hyperfine splitting to the isotropic values because of the complicated angular relationships possible between the **g** and **A** tensors. The EPR spectra of several LMoOXY complexes, including $LMoOCl_2$, $LMoO(SEt)_2$, $LMoO(OMe)_2$, and $LMoO(NCS)_2$, have been successfully simulated in C_s symmetry.[32a] However, the spectrum of $LMoO(SPh)_2$ could not be satisfactorily simulated by assuming C_s symmetry, suggesting that the C_1 coordination symmetry observed for $LMoO(SPh)_2$ in the solid state (vide supra) persists in solution. A detailed analysis of the **g** and **A** tensors for the compounds where X = Y and X is a monodentate ligand conferring monoclinic symmetry on the molecule will be presented elsewhere.[32]

Electronic Absorption Spectra and Infrared Spectra. The electronic spectra of the compounds in 1,2-dichloroethane solution are summarized in Table VI. No simple trends or correlations of the positions of the band maxima with changes of X or Y are apparent. However, on the basis of the molar extinction coefficient of the first (lowest energy) band in the spectrum, the compounds fall into two groups. The first group ($\epsilon_1 < 100$) involves monodentate ligands in which X and Y are chloride, oxygen donors, or thiocyanate. The value of ϵ_1 suggests that this transition is essentially d → d in character. A similar band occurs in the range 12 500–16 000 cm^{-1} in systems such as $[MoOCl_4]^-$, $[MoOCl_4H_2O]^-$, and $MoOCl_3Z_2$ (Z = triphenylphosphine oxide or tris(dimethylamino)phosphine oxide),[24,33-40] which is attributable to

(28) (a) Lamy, M. T.; Gutteridge, S.; Bray, R. C. *Biochem. J.* **1980**, *185*, 397–403. (b) Vincent, S. P.; Bray, R. C. *Biochem. J.* **1978**, *171*, 639–647. (c) Bray, R. C.; Barber, M. J.; Lowe, D. J. *Biochem. J.* **1978**, *171*, 653–658.
(29) Hawkes, T. R.; Bray, R. C. *Biochem. J.* **1984**, *222*, 587–600.
(30) Pariyadath, N.; Newton, W. E.; Stiefel, E. I. *J. Am. Chem. Soc.* **1976**, *98*, 5388–5390.
(31) Rodrigues, C. G.; Farchione, F.; Hanson, G. R.; Wilson, G. L.; O'Connor, M. J.; Wedd, A. G. *Chem. Uses Molybdenum* **1985**, *5*, 55.
(32) (a) Collison, D.; Mabbs, F. E.; Enemark, J. H.; Cleland, W. E., Jr. *Polyhedron* **1986**, *5*, 423–425. (b) Collison, D.; Mabbs, F. E.; Cleland, W. E., Jr.; Enemark, J. H., to be submitted for publication.

Table VI. Electronic Absorption Spectra for LMoOXY Compounds[a]

compd	E_{max}, 10^3 cm^{-1} (ϵ, 10^3 L mol^{-1} cm^{-1})
$LMoOCl_2$ (**1**)	14.18 (0.05), 22.99 (sh, 1.00), 29.67 (5.20)
$LMoO(NCS)_2$ (**2**)	13.62 (0.06), 18.69 (7.30), 21.41 (8.60)
$LMoO(N_3)_2$ (**3**)	13.99 (0.04), 21.28 (sh, 1.61), 25.77 (sh, 3.70)
$LMoO(OMe)_2$ (**4**)	12.99 (0.09), 20.83 (sh, 0.006)
$LMoO(OPh)_2$ (**5**)	13.33 (0.08), 20.83 (sh ~1.44)
$LMoO(SEt)_2$ (**6**)	13.93 (0.36), 16.67 (sh, ~0.34), 25.0 (sh, ~14.30)
$LMoO(SPh)_2$ (**7**)	13.61 (1.65), 16.23 (sh, ~1.40), 22.62 (sh, ~4.10), 26.60 (15.90)
LMoO(Cl,OMe) (**8**)	12.90 (0.03), 20.83 (sh, ~0.006)
LMoO(Cl,OPh) (**9**)	13.16 (0.1), 19.23 (1.79), 28.57 (sh, ~5.80)
LMoO(Cl,SEt) (**10**)	15.50 (0.41), 27.93 (1.87)
LMoO(Cl,SPh) (**11**)	14.20 (1.68), 25.52 (6.40)
LMoO(1-O,O) (**12**)	15.63 (0.02), 19.05 (0.02), 28.74 (3.94)
LMoO(1-O,S) (**13**)	16.53 (0.13), 27.03 (sh, ~2.60), 31.15 (4.10)
LMoO(1-S,S) (**14**)	11.79 (0.16), 15.50 (0.22), 20.00 (sh, ~0.57), 23.53 (sh, ~2.20), 28.17 (3.39)
LMoO(2-O,O) (**15**)	15.11 (0.19), 29.41 (sh, ~4.30)
LMoO(2-O,NH) (**16**)	11.36 (0.17), 20.12 (sh, ~1.30), 25.13 (sh, ~3.53)
LMoO(2-O,S) (**17**)	11.61 (0.20), 23.98 (sh, ~2.64), 27.78 (3.87)
LMoO(2-S,S)[b] (**18**)	9.01 (0.52), 12.99 (0.39), 19.65 (sh, ~1.70), 24.88 (7.40), 27.40 (sh, ~6.05)
LMoO(2-S,NH) (**19**)	8.85 (0.25), 19.84 (sh, ~1.30), 26.60 (8.80)

[a] 1,2-$C_2H_4Cl_2$ solution; sh = shoulder. [b] 2-S,S = toluenedithiolate.

a d → d transition. The second group of compounds have $\epsilon_1 > 100$ for the first band in the electronic spectrum, suggesting charge-transfer character for the transition. Compounds in this group have either a sulfur donor atom or donor atoms directly attached to an aromatic ring. The presence of sulfur donor atoms and a high value of ϵ_1 for a relatively low energy transition is similar to the situation in $[MoO(SPh)_4]^-$, where the first band is at 16 720 cm^{-1} with $\epsilon_1 = 6600$.[41]

It should be possible to correlate trends in the principal g values with changes in the electronic absorption spectra by using eq 5,[42,43] where ξ_{Mo} is the single-electron spin–orbit coupling constant for an electron in a metal d orbital, ΔE^* is the energy associated with a d → d transition, and ΔE is the energy associated with a single-electron excitation from a filled molecular orbital of mainly ligand character to the ground state. The forms of the constants

$$g_i = 2.0023 - \frac{\xi_{Mo}F}{\Delta E^*} + \frac{\xi_{Mo}G}{\Delta E} \qquad (5)$$

F and G are described elsewhere.[42,43] Unfortunately, no trends based on changes in the energies of bands are discernible. However, at a qualitative level it is possible to group $\langle g \rangle$, $^1/_2(g_1 + g_2)$, and $\langle A \rangle$ for the compounds on the same basis as that used for the electronic absorption spectra. With the exception of LMoO(1-O,O), compounds for which $\epsilon_1 > 100$ for the first band in the electronic absorption spectrum also have $\langle g \rangle > 1.950$, $^1/_2(g_1 + g_2) > 1.960$, and $\langle A \rangle < 40 \times 10^{-4}$ cm^{-1}, with g_1 in particular often being close to 2.0023. In contrast to this, compounds with $\epsilon_1 < 100$ have $\langle g \rangle < 1.950$, $^1/_2(g_1 + g_2) < 1.960$, $g_1 < 1.970$, and $\langle A \rangle > 40 \times 10^{-4}$ cm^{-1}. The form of eq 5 suggests that the charge-transfer contribution to a particular g value could be comparable to or even outweigh the contribution from the d → d term. It would appear that for the LMoOXY compounds such a situation obtains when there is at least one sulfur donor atom or when the donor atoms are directly attached to a benzene ring. Thus, to this qualitative extent the electronic absorption spectra and the g values are compatible with each other.

Table VII. Electrochemical Data for LMoOXY Complexes[a,b]

compd	E, V	ΔE_p, mV	i_{pa}/i_{pc}
$LMoOCl_2$ (**1**)	−0.251	90	0.92
$LMoO(NCS)_2$ (**2**)	+0.123	86	1.00
$LMoO(N_3)_2$ (**3**)	−0.308	100	0.95
$LMoO(OMe)_2$ (**4**)	−1.100	90	0.94
$LMoO(OPh)_2$ (**5**)	−0.877	117	0.90
$LMoO(SEt)_2$ (**6**)	−0.530	110	1.02
$LMoO(SPh)_2$ (**7**)	−0.282	64	1.00
LMoO(Cl,OMe) (**8**)	−0.840	155	0.88
LMoO(Cl,OPh) (**9**)	−0.593	137	0.98
LMoO(Cl,SEt) (**10**)	−0.437	102	1.03
LMoO(Cl,SPh) (**11**)	−0.331	71	1.00
LMoO(1-O,O) (**12**)	−1.140	180	0.98
LMoO(1-O,S) (**13**)	−0.757	96	0.97
LMoO(1-S,S) (**14**)	−0.334	55	1.00
LMoO(2-O,O) (**15**)	−0.661	71	1.03
LMoO(2-O,NH) (**16**)	−0.793	77	0.97
LMoO(2-O,S) (**17**)	−0.410	97	0.90
LMoO(2-S,S)[c] (**18**)	−0.280	66	1.00
LMoO(2-S,NH) (**19**)	−0.497	80	1.03

[a] Conditions: cyclic voltametry, Pt electrode, 1–2 mM solutions in MeCN, 0.1 M Bu_4NBF_4 supporting electrolyte. [b] Potentials vs. Ag/AgCl, 23 °C. [c] 2-S,S = toluenedithiolate.

The infrared spectra of the complexes (KBr disk) show the characteristic bands for the hydrotris(3,5-dimethyl-1-pyrazolyl)borate group, metal–ligand vibrations, and a strong Mo=O band. The last vibration ranges from 910 cm^{-1} for LMoO(2-S,NH) to 960 cm^{-1} for $LMoOCl_2$, but the observed Mo=O frequencies show no simple correlation with the energy of the first electronic absorption band, with the reduction potential, or with $\langle g \rangle$. For the LMoO(2-X,Y) complexes ν(Mo=O) ranges from 940 to 910 cm^{-1} and follows the order 2-O,O > 2-O,S > 2-S,S > 2-O,NH > 2-S,NH.

Electrochemistry. The electrochemical behavior of the LMoOXY complexes was examined by cyclic voltammetry and controlled-potential coulometry. All complexes exhibited quasi-reversible one-electron reductions (Table VII) as demonstrated by $i_{pa}/i_{pc} \cong 1.0$, corresponding to formation of the analogous Mo(IV) monoanion. The ΔE_p values range from the theoretical value of 59 mV to 180 mV at a scan rate of 100 mV/s; all approach the theoretical 59 mV at slower scan rates.[44] Similar results have been obtained for various other $[MoO]^{3+}$ complexes,[45] although few mononuclear $[MoO]^{3+}$ complexes are known with other than halide ligands. Controlled-potential coulometry for $LMoO(SPh)_2$ gave 0.96 e/Mo, verifying the one-electron nature of the reductions. The wide range of the reduction potentials of these complexes (~1.3 V) indicates the sensitivity of the reduction potential of the $[LMoO]^{2+}$ core to the nature of the remaining two ligands. The sensitivity of the electronic and EPR spectra to changes in the X and Y ligands was noted above.

Comparison of the reduction potentials for the complexes of monodentate ligands indicates reduction potentials increase in the order OR < SR ≈ N_3 < Cl < NCS. Corresponding SR and OR complexes show a large difference (viz. ~600 mV between $LMoO(SPh)_2$ and $LMoO(OPh)_2$). This behavior is not unexpected and is found for the reduction potentials of other oxo–Mo complexes upon substitution of O for S in complexes with otherwise

(33) Piovesana, O.; Furlani, C. *Inorg. Nucl. Chem. Lett.* **1967**, *3*, 535–538.
(34) Rillema, P. D.; Brubaker, C. H., Jr. *Inorg. Chem.* **1969**, *8*, 1645–1649.
(35) Sabat, H.; Rudolf, M. F.; Jerowska-Trzebiatowska, B. *Inorg. Chim. Acta* **1973**, *7*, 365–369.
(36) Kon, H.; Sharpless, N. E. *J. Chem. Phys.* **1965**, *42*, 906–909.
(37) Garner, C. D.; Lambert, P.; Mabbs, F. E.; King, T. J. *J. Chem. Soc., Dalton Trans.* **1977**, 1191–1198.
(38) Horner, S. M.; Tyree, S. Y. *Inorg. Chem.* **1962**, *1*, 122; *Inorg. Nucl. Chem. Lett.* **1965**, *1*, 43–45.
(39) Garner, C. D.; Hill, L. H.; Mabbs, F. E.; McFadden, D. L.; McPhail, A. T. *J. Chem. Soc., Dalton Trans.* **1977**, 1202–1207.
(40) Winkler, J. R.; Gray, H. B. *Comments Inorg. Chem.* **1981**, *1*, 257–263.
(41) Boyd, I. W.; Dance, I. G.; Murray, K. S.; Wedd, A. G. *Aust. J. Chem.* **1978**, *31*, 279–284.
(42) (a) Garner, C. D.; Hillier, I. H.; Mabbs, F. E.; Taylor, C.; Guest, M. F. *J. Chem. Soc., Dalton Trans.* **1976**, 2258–2261. (b) Garner, C. D.; Mabbs, F. E. *J. Inorg. Nucl. Chem.* **1979**, *41*, 1125–1127.
(43) Glarum, S. H. *J. Chem. Phys.* **1963**, *39*, 3141–3144.
(44) Nicholson, R. S.; Shain, I. *Anal. Chem.* **1964**, *36*, 706–723.
(45) (a) Taylor, R. D.; Street, J. P.; Minelli, M.; Spence, J. T. *Inorg. Chem.* **1978**, *17*, 3207–3211. (b) Bradbury, J. R.; Hanson, G. R.; Boyd, I. W.; Gheller, S. F.; Wedd, A. G.; Murray, K. S.; Bond, A. M. *Chem. Uses Molybdenum* **1979**, *3*, 300–309.

Table VIII. Mass Spectral Data for LMoOXY Compounds

compd	mol wt	peak max of multiplets
$LMoOCl_2$ (**1**)	480	481,[a] 444,[b] 411,[c] 384,[d] 351
$LMoO(NCS)_2$ (**2**)	525	527,[a] 469,[b] 440,[d] 409,[c] 371
$LMoO(N_3)_2$ (**3**)	493	495,[a] 451,[b] 426, 409[c]
$LMoO(OMe)_2$ (**4**)	471	477,[a] 446,[b] 411,[c] 382,[d] 364
$LMoO(OPh)_2$ (**5**)	595	597,[a] 504,[b,d] 446, 408,[c] 367
$LMoO(SEt)_2$ (**6**)	531	532,[a] 504, 471,[b] 443,[d] 427, 411[c]
$LMoO(SPh)_2$ (**7**)	627	628,[a] 520,[b] 490, 446, 424, 411[c]
LMoO(Cl,OMe) (**8**)	479	477,[a] 445,[b] 408,[c] 380,[d] 367, 351
LMoO(Cl,OPh) (**9**)	537	539,[a] 504,[b] 446,[d] 409,[c] 351
LMoO(Cl,SPh) (**10**)	554	555,[a] 520,[b] 481, 446,[d] 429, 409,[c] 386, 351
LMoO(Cl,SEt) (**11**)	505	507,[a] 446,[b] 406,[c,d] 391, 365, 351
LMoO(1-O,O) (**12**)	469	469,[a] 411[c]
LMoO(1-O,S) (**13**)	501	503,[a] 441, 411,[c,d] 379
LMoO(1-S,S) (**14**)	485	486,[a] 457, 411,[c] 391[d]
LMoO(2-O,O) (**15**)	517	516,[a] 423,[d] 409[c]
LMoO(2-O,NH) (**16**)	516	518,[a] 421,[d] 406,[c] 381
LMoO(2-O,S) (**17**)	533	535,[a], 438,[d] 409,[c] 360
LMoO(2-S,S)[e] (**18**)	563	565,[a] 469,[d] 411,[c] 363
LMoO(2-S,NH) (**19**)	532	532,[a] 438,[d] 408[c]

[a] Parent ion peak. [b] Parent – X (or Y). [c] Parent – (X,Y) occurs with a maximum value of 406–412. [d] Parent – pyrazole. [e] 2-S,S = toluenedithiolate.

identical ligands.[45a,46] Examination of the data for the corresponding pairs of LMoO(1-X,Y) and LMoO(2-X,Y) complexes shows that the LMoO(2-X,Y) complexes are more easily reduced than analogous LMoO(1-X,Y) complexes. This may be due to participation of the aromatic ring of the 2-X,Y chelates in the reduction process or to the ability of the aromatic ring to delocalize the negative charge on the reduced compound.

The Mo(V)/Mo(IV) reduction potentials for $LMoO(SR)_2$ complexes in MeCN fall into a relatively narrow range (−0.280 to −0.530 V vs. Ag/AgCl, −83 to −333 mV vs. NHE). These potentials cannot be directly compared to the Mo(V)/Mo(IV) potentials for enzymes because of effects arising from the differing solvent systems. The tabulated Mo(V)/Mo(IV) potentials for molybdenum enzymes range from +220 to −530 mV,[7] and the value for sulfite oxidase is −163 mV.[7]

Mass Spectroscopy. The LMoOXY compounds were also characterized by mass spectroscopy. Table VIII demonstrates the suitability of the technique. The relative atomic mass of each compound is based upon a rounded sum of relative atomic masses, and only ions of mass greater than 350 have been included. The mass numbers in Table VIII refer to the peak of maximum intensity within a multiplet. The multiplets mainly arise from distribution of molybdenum and boron isotopes in the LMoO moiety. The parent ion of each compound has been observed. For compounds with monodentate X and Y ligands, fragments corresponding to the loss of X or Y were identified. For both LMoOXY and LMoO(1-X,Y) the ion $[LMoO]^+$ was also observed. In addition, most compounds show features assignable to loss of one pyrazole ring.

Conclusions. The molybdenum(V) states of "oxo-type" molybdoenzymes have been extensively investigated by EPR techniques for over 25 years.[47] However, interpretation of the wealth of EPR data has been hampered by the lack of well-characterized series of Mo(V) complexes. The wide range of oxo–molybdenum(V) complexes stabilized by the hydrotris(3,5-dimethyl-1-pyrazolyl)borate ligand (L) provides an excellent opportunity to investigate the effect of systematic ligand variations on the spectroscopic properties and reduction potentials of mononuclear oxo–Mo(V) centers. The EPR and electrochemical data for LMoOXY complexes confirm that oxo–Mo(V) centers containing two thiolate ligands most closely match related values for the enzymes.[2,7,11]

The low symmetry of the LMoOXY complexes makes a detailed interpretation of their EPR spectra difficult. The EPR spectrum of $LMoOCl_2$ has been successfully simulated by assuming monoclinic (C_s) symmetry,[32] but a general analysis of the EPR spectra of the LMoOXY complexes will require data from dilute single crystals. Efforts to prepare appropriate host lattice complexes are in progress.

Finally, the extensive series of LMoOXY complexes provide an excellent opportunity for investigating Mo(V/IV) oxidation–reduction processes (reaction B, Scheme I), the kinetics of ligand substitution of mononuclear oxo–molybdenum(V) compounds, and X-ray absorption spectroscopy of Mo(V) compounds. These studies will be the subject of future publications.

Acknowledgment. We thank J. King for experimental assistance. We acknowledge helpful discussions with Profs. J. T. Spence and C. D. Garner, Dr. S. A. Roberts, and M. T. Ashby. Dr. C. P. Marabella carried out several preliminary investigations. We gratefully acknowledge financial support from the National Institutes of Health, the North Atlantic Treaty Organization, and the SERC, U.K. (to D.C. and F.E.M.).

Supplementary Material Available: Listings of anisotropic thermal parameters and hydrogen atom fractional coordinates for $HB(Me_2pz)_3MoO(SPh)_2$ (2 pages); a listing of structure factors (17 pages). Ordering information is given on any current masthead page.

(46) (a) Spence, J. T. *Chem. Uses Molybdenum* **1979**, *3*, 237–244. (b) Berg, J. M.; Holm, R. H. *J. Am. Chem. Soc.* **1985**, *107*, 917–925. (c) Topich, J.; Lyon, J. T., III. *Polyhedron* **1984**, *3*, 55–60. (d) Boyd, I. W.; Spence, J. T. *Inorg. Chem.* **1982**, *21*, 1602–1606.

(47) Bray, R. C.; Malstrom, B. G.; Vanngard, T. *Biochem. J.* **1959**, *73*, 193–197.